Appl. Math. J. Chinese Univ.
2026, 41(2): 269-285

New multisoliton wave solutions in elastic inhomogeneous fractional-order Murnaghan's rod model with stability analysis

Ananya Tripathy[1] Subhadarshan Sahoo[2,*]

Abstract. In this paper, the new solitary wave solutions of the fractional doubly dispersive equation (FDDE) are investigated. These solutions are used in demonstrating wave transmission in elastic inhomogeneous Murnaghan's rod. A very effective method, known as the unified method, is used here to obtain these solutions. In different conditions, the obtained solutions exhibit different pulse patterns including bright, periodic, combined bright-dark, two-soliton interaction, three-soliton interaction, five-soliton interaction, w-shaped, m-shaped, and u-shaped solutions. These physical characteristics are thoroughly investigated by the graphical representation under different values of the parameters which shows the reliability and productivity of the proposed method. In addition, linear stability analysis is applied to analyse the stability of the considered model. The novel aspect of this study is that the investigated model has never been studied by using the proposed method, and the resulting solutions have never been accomplished previously.

§1 Introduction

Nonlinear phenomena are extremely important in explaining the behaviour of physical properties in real-world applications. To gain a better understanding of its application aspects, partial differential equations (PDEs) are used to model the problems [13]. Fractional partial differential equations (FPDEs) cover the modeling of nonlinear phenomena in fractional order means and the behaviour of the model at each point along with non-local properties [24], which has recently gained popularity among academics [18]. Emerging interest in it draws the attention of academics to investigate its behaviour and significance in various fields of science, as well as its applications. The behaviour of nonlinear phenomena can be predicted and many other

Received: 2022-09-01. Revised: 2023-11-14.
MR Subject Classification: 34A08, 34A34, 35A24, 35R11, 26A33.
Keywords: fractional doubly dispersive equation (FDDE), the unified method, solitary wave solutions, Caputo's fractional derivative, stability analysis.
Digital Object Identifier(DOI): https://doi.org/10.1007/s11766-026-4833-0.
*Corresponding author.

valuable details can be discovered by determining its exact analytical solutions. It can be beneficial in various areas including long surface gravity waves [23], birefringent nano-fibers [26], mass-spring-damping systems [24], crystal lattice theory [33], quasi-monochromatic medium [14], elastic circular rod [11], solid physics [12] and many others. Among the various mathematical models [8, 9, 10, 15, 32], the doubly dispersive equation (DDE) [17] is a crucial model which explains the pulse proliferation in Murnaghan's rod. The fractional doubly dispersive model for wave transmission in a nonlinear elastic inhomogeneous Murnaghan's rod [17] is stated as

$$D_t^{2\alpha}W - \frac{F}{\theta_0}D_x^{2\alpha}W - \frac{\epsilon_0}{2}\left[\frac{1}{\theta_0}\left(l_0\beta_0 D_x^{2\alpha}W^2 + \theta_0\nu_0^2 D_{tx}^{4\alpha}W - b\delta_0\nu_0^2 D_x^{4\alpha}W\right)\right] = 0, \quad 0 < \alpha \leq 1, \tag{1}$$

where $W = W(x,t)$ is a function of x (spatial variable) and t (temporal variable). Here, $b = \dfrac{M}{F} < 1$ and $l_0 = \dfrac{B}{F}$ are combinations of the constant scale factors. ϵ_0 is the small parameter. The parameters β_0 and θ_0 are used for the representation of nonlinearity and density terms respectively. ν_0 is the poisson coefficient and $\delta_0 = \dfrac{F}{2\,(1+\nu_0)}$.

As the considered model is a relatively new area of study, there is a growing interest in analysing its functionality. Till now, very little research has been done on eq.(1), which means it still needs much more exploration. Cattani et al. [3] studied the integer-order form of eq.(1) by applying the extended sinh-Gordon equation expansion method and the modified $\exp(-\psi(\zeta))$-expansion function method and found various topological and non-topological solutions. The blow-up solutions and global existence of the DDE have been done by Erbay et al. [5]. Dusunceli et al. [4] used the improved Bernoulli sub-equation function method to get the singular soliton solutions of the integer-order DDE. Silambarasan et al. [27] applied the F-expansion method to the DDE and obtained non-topological elliptic function solutions. The sine-Gordon expansion method is used by Yel [31] to achieve other varieties of solitary wave solutions.

Recently, Rani et al. [17] examined eq.(1) by utilizing the improved generalized Riccati equation method and yielded a variety of solitary wave solutions. It is clear from the preceding literature that only one study [17] has been conducted on the FDDE, which serves as a motivation to investigate its physical significance in a fractional sense. The novelty of this study is the resulting solutions that are of various types and completely new, which also shows the robustness of the method.

The robustness and stability of soliton solutions are crucial in the investigation of nonlinear phenomena in various physical models. These can be attained by locating the exact analytical solutions by various effective techniques such as the extended (G'/G)-expansion [25], the sigmoid function method [28], the direct integral method [30], the new sub-equation method [29], the modified homotopy analysis method [19], and the unified method [21, 22, 16, 1].

The main motivation of this work is to analyse the behaviour of the pulse propagation in the nonlinear fractional inhomogeneous doubly dispersive model by the unified method [16, 21] and to scrutinize the FDDE's stability by linear stability analysis [7, 6, 2]. Here, the motivation behind considering the Caputo fractional derivative form of the DDE is that it accounts for the memory effect as well as the non-local properties that characterize the model's behaviour at

each point of time.

The following is the paper's outline. The Caputo fractional derivative is defined in Section 2. Section 3 discusses the mathematical analysis of the FDDE, while Section 4 covers the procedure and execution of the proposed method. Section 5 includes a graphical representation of the attained solutions including their dynamics by using two-dimensional (2D), three-dimensional (3D), and contour graphics. Section 6 contains an analysis of the stability of eq.(1), and the paper concludes with the conclusion addressed in Section 7.

§2 Caputo fractional derivative

In this section, we have written the definition of the fractional derivative in the Caputo sense [20, 18].

Assume that g is the lowest integer considerably larger than α. Then the Caputo fractional derivative of order α is stated as

$$D_t^{\alpha}(h(t)) = \begin{cases} \dfrac{1}{\Gamma(g-\alpha)} \displaystyle\int_0^t (t-\varsigma)^{g-\alpha-1} \frac{d^g}{d\varsigma^g} h(\varsigma) d\varsigma, & g-1 < \alpha < g, g \in N, \\ \dfrac{d^g}{d\varsigma^g} h(t), & \alpha = g, g \in N. \end{cases} . \tag{2}$$

§3 Mathematical analysis of FDDE

Assume that the fractional transformation necessary to analyze wave propagation in the given model is of the type

$$W(x,t) = \eta(\xi), \quad \text{where} \quad \xi = \frac{x^{\alpha}}{\Gamma(1+\alpha)} - \lambda_0 \frac{t^{\alpha}}{\Gamma(1+\alpha)}. \tag{3}$$

Putting eq.(3) into eq.(1), we get

$$\left(\frac{\lambda_0^2\theta_0 - F}{\theta_0}\right)\eta'' - \frac{\epsilon_0}{\theta_0} l_0 \beta_0 (\eta')^2 - \frac{\epsilon_0}{\theta_0} l_0 \beta_0 \eta\eta'' - \left[\frac{\epsilon_0\lambda_0^2}{2} - \frac{\epsilon_0 b\delta_0}{2\theta_0}\right]\nu_0^2 \eta^{iv} = 0, \tag{4}$$

which, after two times integration with respect to ξ, yields

$$2\left(\lambda_0^2\theta_0 - F\right)\eta - \epsilon_0 l_0 \beta_0 \eta^2 - \epsilon_0 \nu_0^2 \left(\lambda_0^2\theta_0 - b\delta_0\right)\eta'' = 0. \tag{5}$$

§4 Proposed method

In this part, we have addressed the unified method's [21, 22, 16, 1] approach and implementation in order to achieve novel exact analytical solutions.

4.1 The procedure of the proposed method

Here, we have recalled the procedure of the proposed method.

Step-1:

Suppose the solutions of eq.(5) can be expressed in two forms, polynomial function and rational function solutions.

(a) Polynomial function solution

Let, eq.(5) has solutions in the form of polynomial function as

$$\eta(\xi) = \sum_{i=0}^{n} c_i \phi^i(\xi), \tag{6}$$

where $\phi(\xi)$ holds

$$[\phi'(\xi)]^\sigma = \sum_{i=0}^{\sigma k} d_i \phi^i(\xi), \quad \sigma = 1, 2. \tag{7}$$

Here, c_i and d_i are unknown constants to be determined later. By applying the homogeneous balancing principle, a relation between n and k can be achieved in addition to the consistency condition.

(b) Rational function solution

Let, eq.(5) has solutions in the form of rational function as

$$\eta(\xi) = \frac{\sum_{i=0}^{n} c_i \phi^i(\xi)}{\sum_{i=0}^{r} d_i \phi^i(\xi)}, \quad n \geq r, \tag{8}$$

where $\phi(\xi)$ holds

$$[\phi'(\xi)]^\sigma = \sum_{i=0}^{\sigma k} f_i \phi^i(\xi), \quad \sigma = 1, 2. \tag{9}$$

Here, c_i, d_i, and f_i are unknown parameters to be found later. The connection between n, r and k with the consistency condition can be found with the help of the balancing principle.

Step-2:

Applying eq.(6) with eq.(7) and eq.(8) with eq.(9) into eq.(5) results in an algebraic set of equations. An overdetermined set of equations can be created by equating the gathered coefficients of $\phi(\xi)$ to zero.

Step-3:

The respective forms of the solutions of the given model can be reached by solving the equations found in the previous step and implementing the values of the constants.

4.2 Application of the proposed method

Here, we have applied the suggested method as discussed in the previous section to achieve new waveform solutions for the FDDE. The obtained solutions are categorized into two sections, polynomial and rational function solutions.

4.2.1 Polynomial function solutions

Proceeding with the steps of the considered method mentioned in subsec.4.1, we get, deg. $\left[\eta^2\right]$ = deg.$[\eta'']$ $\Rightarrow n = 2(k-1), \forall k \geq 2$.

Also, the consistency condition is $k - 3 \leq 2$ for $k = 2, 3, 4, 5$, which means eq.(5) passes the Painlevé test [1].

(I) For $k = 2$ and $\sigma = 1$:

Here, $n = 2(k-1) = 2(2-1) = 2$. So, eq.(6) becomes

$$\eta(\xi) = c_0 + c_1\phi(\xi) + c_2\phi^2(\xi), \tag{10}$$

and eq.(7) becomes

$$\phi'(\xi) = d_0 + d_1\phi(\xi) + d_2\phi^2(\xi). \tag{11}$$

Now, substituting eq.(10) and eq.(11) into eq.(5) and equalizing the coefficients of $\phi(\xi)$ to zero, we have a set of algebraic equations which upon solving results in

Set-1:

$$c_1 = \frac{12\nu_0^2\left(-F + b\delta_0 + l_0\beta_0\epsilon_0 c_0\right)d_1 d_2}{l_0\beta_0\left(2 + 3\epsilon_0\nu_0^2 d_1^2\right)}, c_2 = \frac{12\nu_0^2\left(-F + b\delta_0 + l_0\beta_0\epsilon_0 c_0\right)d_2^2}{l_0\beta_0\left(2 + 3\epsilon_0\nu_0^2 d_1^2\right)},$$

$$d_0 = -\frac{2\left(F - b\delta_0\right)\nu_0^2 d_1^2 + l_0\beta_0 c_0\left(2 + \epsilon_0\nu_0^2 d_1^2\right)}{4\nu_0^2\left(F - b\delta_0 - l_0\beta_0\epsilon_0 c_0\right)d_2}, \lambda_0 = \mp\frac{\sqrt{-2F + 2l_0\beta_0\epsilon_0 c_0 - 3b\delta_0\epsilon_0\nu_0^2 d_1^2}}{\sqrt{-\theta_0\left(2 + 3\epsilon_0\nu_0^2 d_1^2\right)}},$$

and the corresponding solution for the negative value of λ_0 is

$$\eta(\xi) = c_0 + 3L\left[d_1 + R_1\right] - 6d_1 L, \tag{12}$$

where

$G = \sqrt{\dfrac{2c_0 l_0\beta_0 + 3d_1^2\left(F - b\delta_0\right)\nu_0^2}{\left(F - b\delta_0 - c_0 l_0\beta_0\epsilon_0\right)\nu_0^2}}$, $d_1^2 - 4d_2 d_0 > 0$, $Q^2 - P^2 > 0$,

$L = \dfrac{\left(-F + b\delta_0 + c_0 l_0\beta_0\epsilon_0\right)\nu_0^2\left[d_1 + R_1\right]}{l_0\beta_0\left(2 + 3d_1^2\epsilon_0\nu_0^2\right)}$ and $R_1 = \dfrac{P\cosh(\xi G)G - \sqrt{P^2 + Q^2}G}{Q + P\sinh(\xi G)}$.

Set-2:

$$c_1 = \frac{4\nu_0^2\left(3F - 3b\delta_0 + l_0\beta_0\epsilon_0 c_0\right)d_1 d_2}{l_0\beta_0\left(-2 + \epsilon_0\nu_0^2 d_1^2\right)}, c_2 = \frac{4\nu_0^2\left(3F - 3b\delta_0 + l_0\beta_0\epsilon_0 c_0\right)d_2^2}{l_0\beta_0\left(-2 + \epsilon_0\nu_0^2 d_1^2\right)},$$

$$d_0 = \frac{l_0\beta_0 c_0\left(-2 + \epsilon_0\nu_0^2 d_1^2\right)}{4\nu_0^2\left(3F - 3b\delta_0 + l_0\beta_0\epsilon_0 c_0\right)d_2}, \lambda_0 = \mp\frac{\sqrt{-6F - 2l_0\beta_0\epsilon_0 c_0 + 3b\delta_0\epsilon_0\nu_0^2 d_1^2}}{\sqrt{-6\theta_0 + 3\epsilon_0\theta_0\nu_0^2 d_1^2}}.$$

According to the method, eq.(11) has 27 different forms of solutions, as mentioned in [17]. So, we are skipping over that section. If we disregard the negative powers of $\phi(\xi)$ in [17], the solutions written in **case-3** and **case-4** in [17] will correspond to our two solution sets. So, keeping in mind that, for the ease of the manuscript, only a few of the solutions that differ from [17] have been written down and presented here.

(II) For $k = 2$ and $\sigma = 2$:

Here, $n = 2(k-1) = 2(2-1) = 2$. So, eq.(6) becomes

$$\eta(\xi) = c_0 + c_1\phi(\xi) + c_2\phi^2(\xi), \tag{13}$$

and eq.(7) becomes

$$\phi'(\xi) = \phi(\xi)\sqrt{d_0 + d_1\phi(\xi) + d_2\phi^2(\xi)}. \tag{14}$$

Now, substituting eq.(13) and eq.(14) into eq.(5) and equalizing the coefficients of $\phi(\xi)$ to zero we have a set of algebraic equations which upon solving results in

Set-1:

$$c_0 = 0, c_1 = \frac{12i\left(F - b\delta_0\right)\nu_0^2\sqrt{d_0}\sqrt{d_2}}{\sqrt{-l_0^2\beta_0^2\left(-2 + \epsilon_0\nu_0^2 d_0\right)^2}}, c_2 = \frac{12\left(F - b\delta_0\right)\nu_0^2 d_2}{l_0\beta_0\left(-2 + \epsilon_0\nu_0^2 d_0\right)},$$

$$d_1=\frac{2il_0\beta_0\sqrt{d_0}\left(-2+\epsilon_0\nu_0^2d_0\right)\sqrt{d_2}}{\sqrt{-l_0^2\beta_0^2\left(-2+\epsilon_0\nu_0^2d_0\right)^2}},\lambda_0=\mp\frac{\sqrt{-2F+b\delta_0\epsilon_0\nu_0^2d_0}}{\sqrt{\theta_0\left(-2+\epsilon_0\nu_0^2d_0\right)}}.$$

Set-2:

$$c_0=0,c_1=-\frac{12i\left(F-b\delta_0\right)\nu_0^2\sqrt{d_0}\sqrt{d_2}}{\sqrt{-l_0^2\beta_0^2\left(-2+\epsilon_0\nu_0^2d_0\right)^2}},c_2=\frac{12\left(F-b\delta_0\right)\nu_0^2d_2}{l_0\beta_0\left(-2+\epsilon_0\nu_0^2d_0\right)},$$

$$d_1=-\frac{2il_0\beta_0\sqrt{d_0}\left(-2+\epsilon_0\nu_0^2d_0\right)\sqrt{d_2}}{\sqrt{-l_0^2\beta_0^2\left(-2+\epsilon_0\nu_0^2d_0\right)^2}},\lambda_0=\pm\frac{\sqrt{-2F+b\delta_0\epsilon_0\nu_0^2d_0}}{\sqrt{\theta_0\left(-2+\epsilon_0\nu_0^2d_0\right)}},$$

and the corresponding solution for the positive value of λ_0 is

$$\eta(\xi)=-\frac{48ie^{\xi\sqrt{d_0}}d_0^{\frac{3}{2}}\sqrt{d_2}\left(F-b\delta_0\right)\nu_0^2\sqrt{-l_0^2\beta_0^2\left(-2+d_0\epsilon_0\nu_0^2\right)^2}}{\left(4ie^{\xi\sqrt{d_0}}\sqrt{d_0}\sqrt{d_2}l_0\beta_0\left(-2+d_0\epsilon_0\nu_0^2\right)+\sqrt{-l_0^2\beta_0^2\left(-2+d_0\epsilon_0\nu_0^2\right)^2}\right)^2}. \tag{15}$$

Set-3:

$$c_0=-\frac{2\left(F-b\delta_0\right)\nu_0^2d_0}{l_0\beta_0\left(2+\epsilon_0\nu_0^2d_0\right)},c_1=-\frac{12i\left(F-b\delta_0\right)\nu_0^2\sqrt{d_0}\sqrt{d_2}}{\sqrt{-l_0^2\beta_0^2\left(2+\epsilon_0\nu_0^2d_0\right)^2}},c_2=-\frac{12\left(F-b\delta_0\right)\nu_0^2d_2}{l_0\beta_0\left(2+\epsilon_0\nu_0^2d_0\right)},$$

$$d_1=\frac{2il_0\beta_0\sqrt{d_0}\left(2+\epsilon_0\nu_0^2d_0\right)\sqrt{d_2}}{\sqrt{-l_0^2\beta_0^2\left(2+\epsilon_0\nu_0^2d_0\right)^2}},\lambda_0=\mp\frac{\sqrt{2F+b\delta_0\epsilon_0\nu_0^2d_0}}{\sqrt{\theta_0\left(2+\epsilon_0\nu_0^2d_0\right)}}.$$

Set-4:

$$c_0=-\frac{2\left(F-b\delta_0\right)\nu_0^2d_0}{l_0\beta_0\left(2+\epsilon_0\nu_0^2d_0\right)},c_1=\frac{12i\left(F-b\delta_0\right)\nu_0^2\sqrt{d_0}\sqrt{d_2}}{\sqrt{-l_0^2\beta_0^2\left(2+\epsilon_0\nu_0^2d_0\right)^2}},c_2=-\frac{12\left(F-b\delta_0\right)\nu_0^2d_2}{l_0\beta_0\left(2+\epsilon_0\nu_0^2d_0\right)},$$

$$d_1=-\frac{2il_0\beta_0\sqrt{d_0}\left(2+\epsilon_0\nu_0^2d_0\right)\sqrt{d_2}}{\sqrt{-l_0^2\beta_0^2\left(2+\epsilon_0\nu_0^2d_0\right)^2}},\lambda_0=\mp\frac{\sqrt{2F+b\delta_0\epsilon_0\nu_0^2d_0}}{\sqrt{\theta_0\left(2+\epsilon_0\nu_0^2d_0\right)}},$$

and the respective solutions for the negative value of λ_0 are

$$\eta_1(\xi)=R_2\left[\left(1+16e^{2\xi\sqrt{d_0}}d_0d_2\right)l_0\beta_0\left(2+d_0\epsilon_0\nu_0^2\right)+16ie^{\xi\sqrt{d_0}}\sqrt{d_0}\sqrt{d_2}\sqrt{-l_0^2\beta_0^2\left(2+d_0\epsilon_0\nu_0^2\right)^2}\right], \tag{16}$$

where

$$R_2=\frac{2d_0\left(F-b\delta_0\right)\nu_0^2}{\left[4ie^{\xi\sqrt{d_0}}\sqrt{d_0}\sqrt{d_2}l_0\beta_0\left(2+d_0\epsilon_0\nu_0^2\right)+\sqrt{-l_0^2\beta_0^2\left(2+d_0\epsilon_0\nu_0^2\right)^2}\right]^2}.$$

$$\begin{aligned}\eta_2(\xi)=&-R_3\left[24\left\{\operatorname{sech}\left(\frac{\xi\sqrt{d_0}}{2}\right)\right\}^4+192\left\{\operatorname{csch}\left(\xi\sqrt{d_0}\right)\right\}^2\left\{\sinh\left(\frac{\xi\sqrt{d_0}}{4}\right)\right\}^4\right]\\&-\frac{2d_0\left(F-b\delta_0\right)\nu_0^2}{l_0\beta_0\left(2+d_0\epsilon_0\nu_0^2\right)}+R_3\left[12\left\{\operatorname{sech}\left(\frac{\xi\sqrt{d_0}}{2}\right)\right\}^2\left\{3+2\tanh\left(\frac{\xi\sqrt{d_0}}{4}\right)\right\}\right],\end{aligned} \tag{17}$$

and

$$R_3=\frac{2d_0\left(F-b\delta_0\right)\nu_0^2}{l_0\beta_0\left(2+d_0\epsilon_0\nu_0^2\right)\left[-3+\tanh\left(\frac{\xi\sqrt{d_0}}{4}\right)\right]^2\left[1+\tanh\left(\frac{\xi\sqrt{d_0}}{4}\right)\right]^2}.$$

4.2.2 Rational function solutions

Proceeding with the steps of the considered method mentioned in subsec.4.1, we get, deg.$\left[\eta^2\right]$ = deg.$[\eta'']$ $\Rightarrow n - r = 2(k-1), \forall k \geq 1$.
Also, the consistency condition is $r + (k-1)2 - k - 2 \leq 2$ for $r \geq 0$ which means eq.(5) passes the Painlevé test [1].

(I) For $k = 1$ (which means $n = r$) and $\sigma = 2$:
Let $n = 1$. So, eq.(8) becomes

$$\eta(\xi) = \frac{c_0 + c_1\phi(\xi)}{d_0 + d_1\phi(\xi)}, \tag{18}$$

and eq.(9) becomes

$$\phi'(\xi) = \sqrt{f_0 + f_1\phi(\xi) + f_2\phi^2(\xi)}. \tag{19}$$

Now, substituting eq.(18) and eq.(19) into eq.(5) and equalizing the coefficients of $\phi(\xi)$ to zero we have a set of algebraic equations.

Set-1:

$$c_0 = -\frac{2\left(F - b\delta_0\right)\nu_0^2\left(4d_1^2f_0 - 4d_0d_1f_1 + d_0^2f_2\left(2 + \epsilon_0\nu_0^2f_2\right)\right)}{l_0\beta_0d_0\left(-4 + \epsilon_0^2\nu_0^4f_2^2\right)}, c_1 = \frac{c_0d_1}{d_0},$$
$$\lambda_0 = \mp\frac{\sqrt{4\left(F - b\delta_0\right)\epsilon_0\nu_0^2d_1\left(d_0f_1 - d_1f_0\right) + d_0^2\left(2 + \epsilon_0\nu_0^2f_2\right)\left(-2F + b\delta_0\epsilon_0\nu_0^2f_2\right)}}{\sqrt{\theta_0d_0^2\left(-4 + \epsilon_0^2\nu_0^4f_2^2\right)}}.$$

Set-2:

$$c_0 = -\frac{3\left(F - b\delta_0\right)\nu_0^2\left(-d_0\left(f_1^2 - 4f_0f_2\right) + f_1L_1\right)}{2l_0\beta_0f_0\left(-2 + \epsilon_0\nu_0^2f_2\right)}, c_1 = 0,$$
$$d_1 = \frac{d_0f_1 - L_1}{2f_0}, \lambda_0 = \mp\frac{\sqrt{-2F + b\delta_0\epsilon_0\nu_0^2f_2}}{\sqrt{\theta_0\left(-2 + \epsilon_0\nu_0^2f_2\right)}}.$$

Set-3:

$$c_0 = -\frac{2\left(F - b\delta_0\right)\nu_0^2d_0f_2}{l_0\beta_0\left(2 + \epsilon_0\nu_0^2f_2\right)}, c_1 = \frac{\left(F - b\delta_0\right)\nu_0^2f_2\left(-d_0f_1 + L_1\right)}{l_0\beta_0f_0\left(2 + \epsilon_0\nu_0^2f_2\right)},$$
$$d_1 = \frac{d_0f_1 - L_1}{2f_0}, \lambda_0 = \mp\frac{\sqrt{2F + b\delta_0\epsilon_0\nu_0^2f_2}}{\sqrt{\theta_0\left(2 + \epsilon_0\nu_0^2f_2\right)}}.$$

Set-4:

$$c_0 = \frac{\left(F - b\delta_0\right)\nu_0^2\left(3f_1L_1 + d_0\left(-3f_1^2 + 8f_0f_2\right)\right)}{2l_0\beta_0f_0\left(2 + \epsilon_0\nu_0^2f_2\right)},$$
$$c_1 = \frac{\left(F - b\delta_0\right)\nu_0^2f_2\left(-d_0f_1 + L_1\right)}{l_0\beta_0f_0\left(2 + \epsilon_0\nu_0^2f_2\right)}, d_1 = \frac{d_0f_1 - L_1}{2f_0}, \lambda_0 = \mp\frac{\sqrt{2F + b\delta_0\epsilon_0\nu_0^2f_2}}{\sqrt{\theta_0\left(2 + \epsilon_0\nu_0^2f_2\right)}},$$

and the respective solution for the negative value of λ_0 is

$$\begin{aligned}\eta(\xi) =& R_4\left[6f_1L_1 + d_0\left(-6f_1^2 + 16f_0f_2\right)\right] \\ &+ R_4\left[e^{-\xi\sqrt{f_2}}\left(e^{2\xi\sqrt{f_2}} - 2e^{\xi\sqrt{f_2}}f_1 + f_1^2 - 4f_0f_2\right)\left\{-d_0f_1 + L_1\right\}\right],\end{aligned} \tag{20}$$

where

$$R_4 = \frac{\dfrac{\left(F - b\delta_0\right)2f_2\nu_0^2}{l_0\beta_0\left(2 + f_2\epsilon_0\nu_0^2\right)}}{\left[8d_0f_0f_2 + \left\{e^{\xi\sqrt{f_2}} - 2f_1 + e^{-\xi\sqrt{f_2}}\left(f_1^2 - 4f_0f_2\right)\right\}\left\{d_0f_1 - L_1\right\}\right]}.$$

Set-5:

$$c_0 = \frac{3\left(F - b\delta_0\right)\nu_0^2\left(d_0\left(f_1^2 - 4f_0f_2\right) + f_1L_1\right)}{2l_0\beta_0f_0\left(-2 + \epsilon_0\nu_0^2f_2\right)}, c_1 = 0,$$
$$d_1 = \frac{d_0f_1 + L_1}{2f_0}, \lambda_0 = \mp\frac{\sqrt{-2F + b\delta_0\epsilon_0\nu_0^2f_2}}{\sqrt{\theta_0\left(-2 + \epsilon_0\nu_0^2f_2\right)}}.$$

Set-6:

$$c_0 = -\frac{2\left(F - b\delta_0\right)\nu_0^2d_0f_2}{l_0\beta_0\left(2 + \epsilon_0\nu_0^2f_2\right)}, c_1 = -\frac{\left(F - b\delta_0\right)\nu_0^2f_2\left(d_0f_1 + L_1\right)}{l_0\beta_0f_0\left(2 + \epsilon_0\nu_0^2f_2\right)},$$
$$d_1 = \frac{d_0f_1 + L_1}{2f_0}, \lambda_0 = \mp\frac{\sqrt{2F + b\delta_0\epsilon_0\nu_0^2f_2}}{\sqrt{\theta_0\left(2 + \epsilon_0\nu_0^2f_2\right)}}.$$

Set-7:

$$c_0 = -\frac{\left(F - b\delta_0\right)\nu_0^2\left(3f_1L_1 + d_0\left(3f_1^2 - 8f_0f_2\right)\right)}{2l_0\beta_0f_0\left(2 + \epsilon_0\nu_0^2f_2\right)},$$
$$c_1 = -\frac{\left(F - b\delta_0\right)\nu_0^2f_2\left(d_0f_1 + L_1\right)}{l_0\beta_0f_0\left(2 + \epsilon_0\nu_0^2f_2\right)}, d_1 = \frac{d_0f_1 + L_1}{2f_0}, \lambda_0 = \mp\frac{\sqrt{2F + b\delta_0\epsilon_0\nu_0^2f_2}}{\sqrt{\theta_0\left(2 + \epsilon_0\nu_0^2f_2\right)}}.$$

In the above solution sets, $L_1 = \sqrt{d_0^2\left(f_1^2 - 4f_0f_2\right)}$.

(II) For $k = 1$ (which means $n = r$) and $\sigma = 2$:

Let $n = 1$. So, eq.(8) becomes

$$\eta(\xi) = \frac{c_0 + c_1\phi(\xi)}{d_0 + d_1\phi(\xi)}, \tag{21}$$

and eq.(9) becomes

$$\phi'(\xi) = \sqrt{f_0^2 - f_2^2\phi^2(\xi)}. \tag{22}$$

Now, substituting eq.(21) and eq.(22) into eq.(5) and equalizing the coefficients of $\phi(\xi)$ to zero, we have a set of algebraic equations.

Set-1:

$$c_0 = -\frac{2\left(F - b\delta_0\right)\nu_0^2\left(4d_1^2f_0^2 + d_0^2f_2^2\left(-2 + \epsilon_0\nu_0^2f_2^2\right)\right)}{l_0\beta_0d_0\left(-4 + \epsilon_0^2\nu_0^4f_2^4\right)}, c_1 = \frac{c_0d_1}{d_0},$$
$$\lambda_0 = \mp\frac{\sqrt{-4\left(F - b\delta_0\right)\epsilon_0\nu_0^2d_1^2f_0^2 + d_0^2\left(-2 + \epsilon_0\nu_0^2f_2^2\right)\left(2F + b\delta_0\epsilon_0\nu_0^2f_2^2\right)}}{\sqrt{\theta_0d_0^2\left(-4 + \epsilon_0^2\nu_0^4f_2^4\right)}}.$$

Set-2:

$$c_0 = -\frac{2\left(F - b\delta_0\right)\nu_0^2d_0f_2^2}{l_0\beta_0\left(-2 + \epsilon_0\nu_0^2f_2^2\right)}, c_1 = -\frac{c_0f_2}{f_0}, d_1 = -\frac{d_0f_2}{f_0}, \lambda_0 = \mp\frac{\sqrt{-2F + b\delta_0\epsilon_0\nu_0^2f_2^2}}{\sqrt{\theta_0\left(-2 + \epsilon_0\nu_0^2f_2^2\right)}}.$$

Set-3:

$$c_0 = \frac{4\left(F - b\delta_0\right)\nu_0^2d_0f_2^2}{l_0\beta_0\left(-2 + \epsilon_0\nu_0^2f_2^2\right)}, c_1 = \frac{2c_0f_2}{f_0}, d_1 = -\frac{d_0f_2}{f_0}, \lambda_0 = \mp\frac{\sqrt{-2F + b\delta_0\epsilon_0\nu_0^2f_2^2}}{\sqrt{\theta_0\left(-2 + \epsilon_0\nu_0^2f_2^2\right)}}.$$

Set-4:

$$c_0 = -\frac{6\left(F - b\delta_0\right)\nu_0^2d_0f_2^2}{l_0\beta_0\left(2 + \epsilon_0\nu_0^2f_2^2\right)}, c_1 = 0, d_1 = -\frac{d_0f_2}{f_0}, \lambda_0 = \mp\frac{\sqrt{2F + b\delta_0\epsilon_0\nu_0^2f_2^2}}{\sqrt{\theta_0\left(2 + \epsilon_0\nu_0^2f_2^2\right)}},$$

and the solution for the negative value of λ_0 becomes

$$\eta(\xi) = -\frac{6\sqrt{\sec(\xi f_2)^2} f_2^2 \left(F - b\delta_0\right) \nu_0^2}{l_0 \beta_0 \left(2 + f_2^2 \epsilon_0 \nu_0^2\right) \left[\sqrt{\sec(\xi f_2)^2} + \tan(\xi f_2)\right]}. \tag{23}$$

Set-5:

$$c_0 = -\frac{2\left(F - b\delta_0\right) \nu_0^2 d_0 f_2^2}{l_0 \beta_0 \left(-2 + \epsilon_0 \nu_0^2 f_2^2\right)}, c_1 = \frac{c_0 f_2}{f_0}, d_1 = \frac{d_0 f_2}{f_0}, \lambda_0 = \mp \frac{\sqrt{-2F + b\delta_0 \epsilon_0 \nu_0^2 f_2^2}}{\sqrt{\theta_0 \left(-2 + \epsilon_0 \nu_0^2 f_2^2\right)}},$$

and the corresponding solution for the negative value of λ_0 is

$$\eta(\xi) = -\frac{2 f_2^2 \left(F - b\delta_0\right) \nu_0^2}{l_0 \beta_0 \left(f_2^2 \epsilon_0 \nu_0^2 - 2\right)}. \tag{24}$$

Set-6:

$$c_0 = \frac{4\left(F - b\delta_0\right) \nu_0^2 d_0 f_2^2}{l_0 \beta_0 \left(-2 + \epsilon_0 \nu_0^2 f_2^2\right)}, c_1 = -\frac{2 c_0 f_2}{f_0}, d_1 = \frac{d_0 f_2}{f_0}, \lambda_0 = \mp \frac{\sqrt{-2F + b\delta_0 \epsilon_0 \nu_0^2 f_2^2}}{\sqrt{\theta_0 \left(-2 + \epsilon_0 \nu_0^2 f_2^2\right)}}.$$

Set-7:

$$c_0 = -\frac{6\left(F - b\delta_0\right) \nu_0^2 d_0 f_2^2}{l_0 \beta_0 \left(2 + \epsilon_0 \nu_0^2 f_2^2\right)}, c_1 = 0, d_1 = \frac{d_0 f_2}{f_0}, \lambda_0 = \mp \frac{\sqrt{2F + b\delta_0 \epsilon_0 \nu_0^2 f_2^2}}{\sqrt{\theta_0 \left(2 + \epsilon_0 \nu_0^2 f_2^2\right)}}.$$

Remark: Only a few of the solutions are listed here for ease of the paper.

§5 Numerical simulation

In this section, the physical meaning of the derived solutions is examined by assigning numerical values to the unknown parameters. It has also been displayed in 2D, 3D, and contour graphics.

5.1 Graphical representation of the solutions

Here, we have graphically displayed the solutions of eq.(12), eq.(15), eq.(16), eq.(17) and eq.(20) for different fractional and other parametric values.

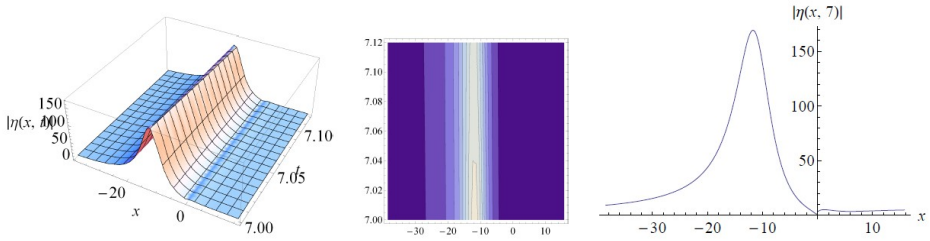

Figure 1. (a) 3D graphics, (b) contour graphics, and (c) 2D graphics of eq.(12) when $\alpha = 0.3$.

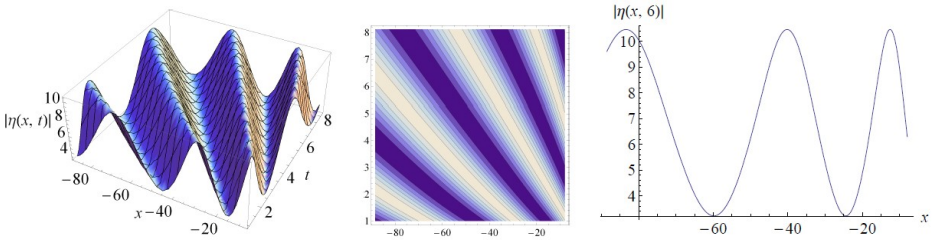

Figure 2. (a) 3D graphics, (b) contour graphics, and (c) 2D graphics of eq.(12) when $\alpha = 0.5$.

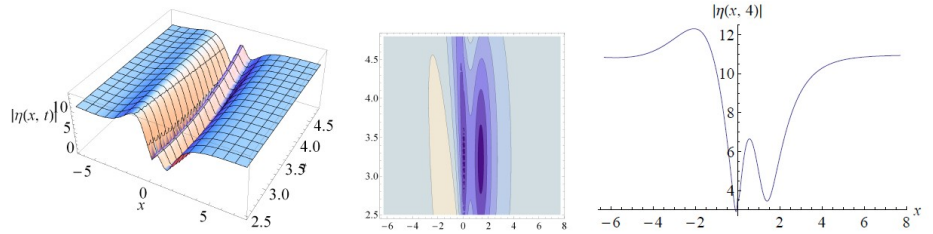

Figure 3. (a) 3D graphics, (b) contour graphics, and (c) 2D graphics of eq.(12) when $\alpha = 0.7$.

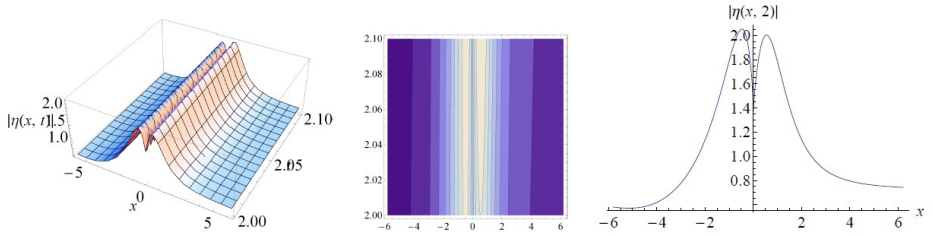

Figure 4. (a) 3D graphics, (b) contour graphics, and (c) 2D graphics of eq.(12) when $\alpha = 0.65$.

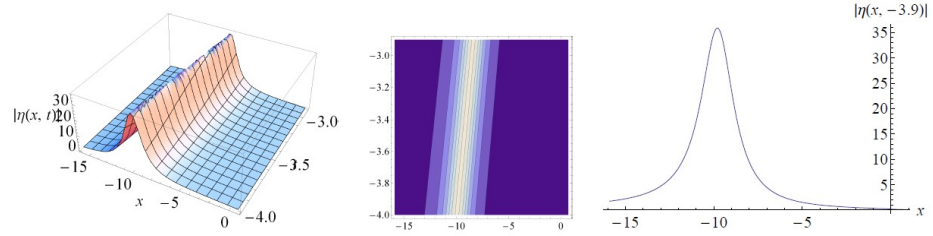

Figure 5. (a) 3D graphics, (b) contour graphics, and (c) 2D graphics of eq.(15) when $\alpha = 0.7$.

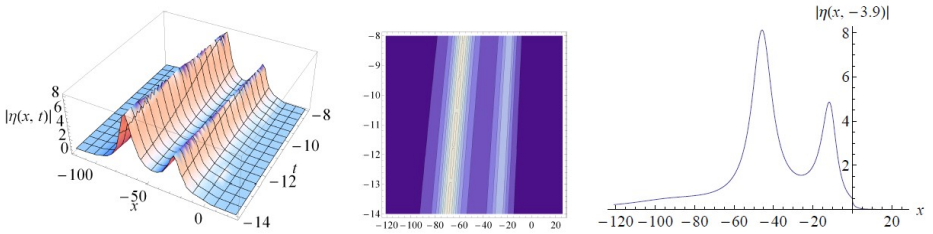

Figure 6. (a) 3D graphics, (b) contour graphics, and (c) 2D graphics of eq.(15) when $\alpha = 0.6$.

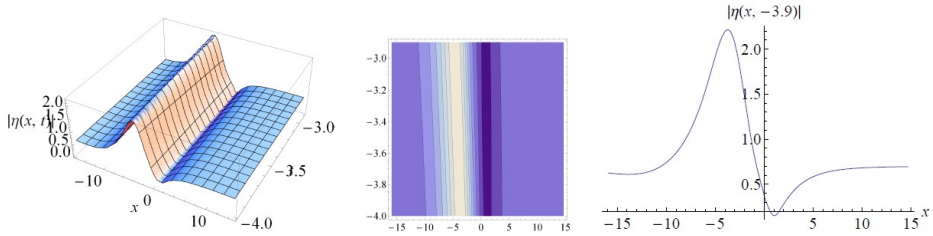

Figure 7. (a) 3D graphics, (b) contour graphics, and (c) 2D graphics of eq.(16) when $\alpha = 0.7$.

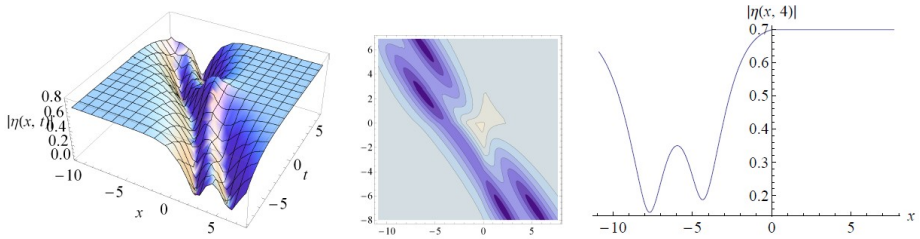

Figure 8. (a) 3D graphics, (b) contour graphics, and (c) 2D graphics of eq.(16) when $\alpha = 0.9$.

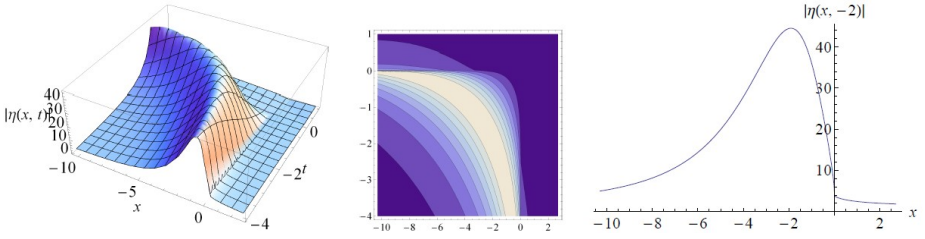

Figure 9. (a) 3D graphics, (b) contour graphics, and (c) 2D graphics of eq.(17) when $\alpha = 0.4$.

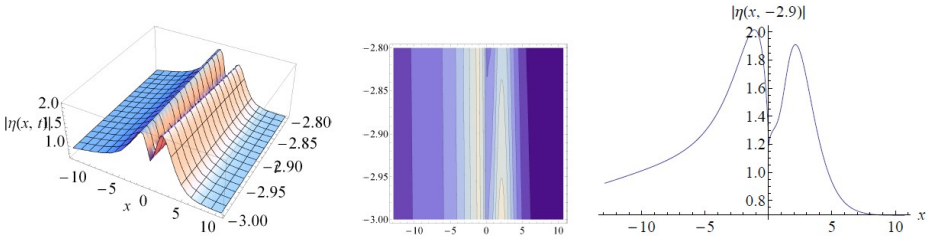

Figure 10. (a) 3D graphics, (b) contour graphics, and (c) 2D graphics of eq.(17) when $\alpha = 0.73$.

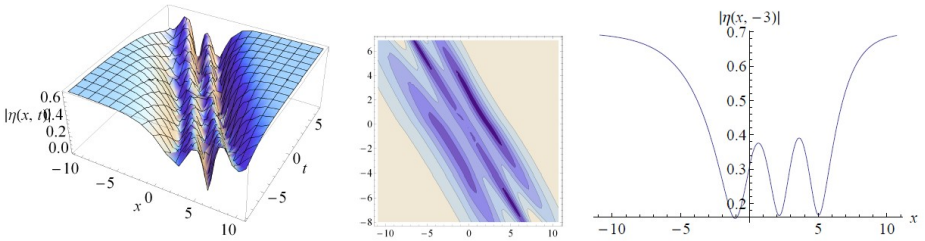

Figure 11. (a) 3D graphics, (b) contour graphics, and (c) 2D graphics of eq.(17) when $\alpha = 0.95$.

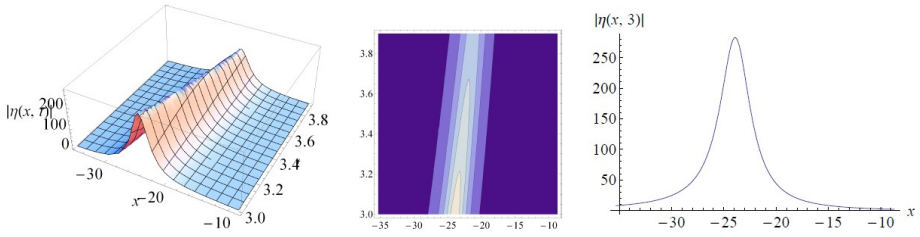

Figure 12. (a) 3D graphics, (b) contour graphics, and (c) 2D graphics of eq.(20) when $\alpha = 0.45$.

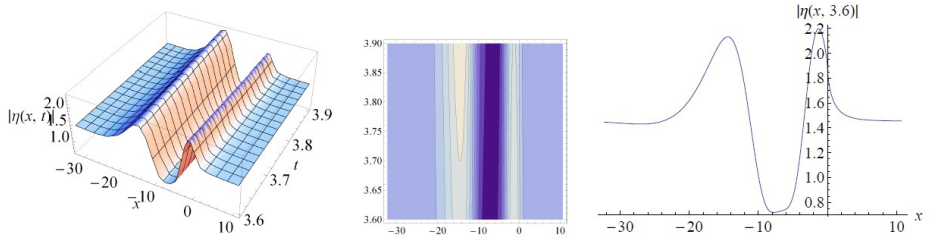

Figure 13. (a) 3D graphics, (b) contour graphics, and (c) 2D graphics of eq.(20) when $\alpha = 0.75$.

5.2 Dynamics of the optical solutions

Here, we have examined and explained the physical properties of the newly achieved analytical solutions using 2D, 3D, and contour graphs. It can be observed that the contour graphics are the 3D graphics on 2D surfaces.

The graphical representation of different forms of eq.(12) under different parametric values is illustrated in Figs.1-4. In Fig.1, it shows the bright solution for the fractional-order $\alpha = 0.3$ within the range $-38.5 \leq x \leq 15.8$ and $7 \leq t \leq 7.12$ while Fig.2 shows the periodic wave solution for the fractional-order $\alpha = 0.5$ in the range $-88.5 \leq x \leq -8$ and $1 \leq t \leq 8.12$.

By decreasing some of the parametric values and increasing the fractional value to 0.7, the w-shaped solution is obtained in the interval $-6.3 \leq x \leq 7.7$ and $2.5 \leq t \leq 4.8$ which is shown in Fig.3. The w-shaped solutions are another variety of dark solutions maintaining their stability during transmission over long distances. Fig.4 depicts the m-shaped solution for the fractional-order $\alpha = 0.65$ within the range $-5.8 \leq x \leq 6.2$ and $2 \leq t \leq 2.1$. The m-shaped solutions are another variety of bright-shaped solutions with an increase in their wave amplitude and zero-intensity background. Comparing these four wave patterns with those obtained in [17], it can be observed that, our solutions are different and new.

The graphical illustration of different wave patterns of eq.(15) is presented in Fig.5 and Fig.6. Fig.5 delineates the bright solution for the fractional-order $\alpha = 0.7$ in the range $-15.9 \leq x \leq 0.7$ and $-4 \leq t \leq -2.9$ while decreasing the fractional value to 0.6, it shows the two-soliton interaction solution in the interval $-120.9 \leq x \leq 25.7$ and $-14 \leq t \leq -8$ which is displayed in Fig.6.

Fig.7 and Fig.8 explain the different pulse patterns of eq.(16). Fig.7 depicts the combined bright-dark solution for the fractional-order $\alpha = 0.7$ in the range $-15.9 \leq x \leq 14.7$ and $-4 \leq t \leq -2.9$ while increasing the fractional value to 0.9, the five-soliton interaction solution within the limit $-10.9 \leq x \leq 7.7$ and $-8 \leq t \leq 6.9$ is achieved which is shown in fig.8. Here, the five-soliton interaction solution shows the combined properties of dark and bright solutions which can be observed from the corresponding contour plot.

Figs.9-11 show the various pulse patterns of eq.(17). Fig.9 shows the slight bending pattern of bright solution during propagation for the fractional-order $\alpha = 0.4$ in the range $-10.3 \leq x \leq 2.7$ and $-4 \leq t \leq 1$. By increasing some of the parametric values and the fractional value to 0.73, it shows the m-shaped solution within the interval $-12.9 \leq x \leq 10.7$ and $-3 \leq t \leq -2.8$ which is displayed in Fig.10. Fig.11 depicts the three-soliton interaction solution for the fractional-order $\alpha = 0.95$ in the range $-10.9 \leq x \leq 10.7$ and $-8 \leq t \leq 6.9$. Here, it demonstrates the properties of the dark solutions.

The graphical representation of different pulse shapes of eq.(20) is displayed in Fig.12 and Fig.13. Fig.12 delineates the properties of bright solution for the fractional-order $\alpha = 0.45$ in the range $-35.3 \leq x \leq -8.7$ and $3 \leq t \leq 3.9$ while Fig.13 delineates the u-shaped solution for the fractional-order $\alpha = 0.75$ in the interval $-32.3 \leq x \leq 10.7$ and $3.6 \leq t \leq 3.9$.

§6 Stability analysis

In this section, we have investigated the stability analysis [7,6,2] of eq.(1) for $\alpha = 1$. And to accomplish so, we have used the perturbed solution as

$$W(x,t) = P_0 + \tau A(x,t), \tag{25}$$

where P_0 is any steady-state solution of eq.(1). Now, by putting eq.(25) into eq.(1), we have

$$\begin{aligned} \tau A_{tt} - \frac{F}{\theta_0}\tau A_{xx} - \frac{\epsilon_0}{2}\left[\frac{1}{\theta_0}\left\{l_0\beta_0\left(2\tau^2 A_x^2 + 2\tau P_0 A_{xx} + 2\tau^2 A A_{xx}\right)\right\}\right] \\ - \frac{\epsilon_0}{2}\left[\frac{1}{\theta_0}\left(\theta_0\nu_0^2\tau A_{xxtt} - b\delta_0\nu_0^2\tau A_{xxxx}\right)\right] = 0, \end{aligned} \tag{26}$$

which upon linearization in τ gives,

$$\tau A_{tt} - \frac{F}{\theta_0}\tau A_{xx} - \frac{\epsilon_0}{2}\left[\frac{1}{\theta_0}\left\{2\tau l_0\beta_0 P_0 A_{xx} + \theta_0\nu_0^2\tau A_{xxtt} - b\delta_0\nu_0^2\tau A_{xxxx}\right\}\right] = 0. \tag{27}$$

Suppose the solution of eq.(27) is in the form,

$$A(x,t) = e^{i(k_1 x + \omega t)}, \tag{28}$$

where k_1 is the normalized wave number and $\omega = \omega(k_1)$ is the dispersion relation. Putting eq.(28) into eq.(27) and solving for ω, we get

$$\omega = \omega(k_1) = -\frac{k_1\sqrt{2F + \epsilon_0\left(2l_0P_0\beta_0 + bk_1^2\delta_0\nu_0^2\right)}}{\sqrt{\theta_0\left(2 + k_1^2\epsilon_0\nu_0^2\right)}}. \tag{29}$$

It is clear from eq.(29) that the real component is negative for all values of k_1. Thus, the dispersion maintains its stability. Now, to obtain the phase velocity $\dfrac{\gamma(k_1)}{k_1}$, we suppose the solution is in the form,

$$A(x,t) = e^{i(k_1 x + \gamma t)}. \tag{30}$$

Substituting eq.(30) into eq.(27) and solving for $\gamma(k_1)$, we get

$$\gamma = \gamma(k_1) = -\frac{k_1\sqrt{2F + \epsilon_0\left(2l_0P_0\beta_0 + bk_1^2\delta_0\nu_0^2\right)}}{\sqrt{\theta_0\left(2 + k_1^2\epsilon_0\nu_0^2\right)}}. \tag{31}$$

Thus, the phase velocity is

$$\frac{\gamma}{k_1} = \frac{\gamma(k_1)}{k_1} = -\frac{\sqrt{2F + \epsilon_0\left(2l_0P_0\beta_0 + bk_1^2\delta_0\nu_0^2\right)}}{\sqrt{\theta_0\left(2 + k_1^2\epsilon_0\nu_0^2\right)}}, \tag{32}$$

and the phase velocity multiplied by two yields the group velocity.

§7 Conclusion

The successful implementation of the unified method to acquire new solitary wave solutions of the FDDE is described in this paper. The wave propagates in a variety of patterns depending on the parametric value including bright, periodic, combined bright-dark, two-soliton interaction, three-soliton interaction, five-soliton interaction, w-shaped, m-shaped, and u-shaped solutions. These properties are examined by using 2D, 3D, and contour graphics, which demonstrate the efficiency of the proposed method. Furthermore, the FDDE's stability is scrutinized by using linear stability analysis. The main originality of this work is that the considered model

has never been studied using the proposed method, and the resulting solutions have never been obtained previously.

Declarations

Conflict of interest The authors declare no conflict of interest. The datasets generated during and/or analysed during the current study are available from the corresponding author on reasonable request.

References

[1] H I Abdel-Gawad. *Towards a Unified Method for Exact Solutions of Evolution Equations. An Application to Reaction Diffusion Equations with Finite Memory Transport*, J Stat Phys, 2012, 147: 506-518.

[2] S Ahmed, R Ashraf, A R Seadawy, et al. *Lump, multi-wave, kinky breathers, interactional solutions and stability analysis for general (2+1)-rth dispersionless Dym equation*, Results Phys, 2021, 25: 104160.

[3] C Cattani, T A Sulaiman, H M Baskonus, et al. *Solitons in an inhomogeneous Murnaghan's rod*, Eur Phys J Plus, 2018, 133(6): 1-11.

[4] F Dusunceli, E Celik, M Askin, et al. *New exact solutions for the doubly dispersive equation using the improved Bernoulli sub-equation function method*, Indian J Phys, 2021, 95(2): 309-314.

[5] H A Erbay, S Erbay, A Erkip. *Thresholds for global existence and blow-up in a general class of doubly dispersive nonlocal wave equations*, Nonlinear Anal Theory Methods Appl, 2014, 95: 313-322.

[6] B Ghanbari, M Inc, A Yusuf, et al. *New solitary wave solutions and stability analysis of the Benney-Luke and the phi-4 equations in mathematical physics*, AIMS math, 2019, 4(6): 1523-1539.

[7] M Inc, A Yusuf, A I Aliyu, et al. *Soliton solutions and stability analysis for some conformable nonlinear partial differential equations in mathematical physics*, Opt Quantum Electron, 2018, 50: 190.

[8] M M A Khater. *Novel computational simulation of the propagation of pulses in optical fibers regarding the dispersion effect*, Int J Mod Phys B, 2023, 37(09): 2350083.

[9] M M A Khater. *In surface tension; gravity-capillary, magneto-acoustic, and shallow water waves' propagation*, Eur Phys J Plus, 2023, 138(4): 320.

[10] M M A Khater. *Prorogation of waves in shallow water through unidirectional Dullin–Gottwald–Holm model; computational simulations*, Int J Mod Phys B, 2023, 37(8): 2350071.

[11] M M A Khater. *Nonlinear elastic circular rod with lateral inertia and finite radius: Dynamical attributive of longitudinal oscillation*, Int J Mod Phys B, 2023, 37(6): 2350052.

[12] M M A Khater. *In solid physics equations, accurate and novel soliton wave structures for heating a single crystal of sodium fluoride*, Int J Mod Phys B, 2023, 37(07): 2350068.

[13] M M A Khater, S H Alfalqi, J F Alzaidi, et al. *Novel soliton wave solutions of a special model of the nonlinear Schrödinger equations with mixed derivatives*, Results Phys, 2023, 47: 106367.

[14] M M A Khater, S H Alfalqi, J F Alzaidi, et al. *Analytically and numerically, dispersive, weakly nonlinear wave packets are presented in a quasi-monochromatic medium*, Results Phys, 2023, 46: 106312.

[15] M M A Khater, X Zhang, R A M Attia. *Accurate computational simulations of perturbed Chen–Lee–Liu equation*, Results Phys, 2023, 45: 106227.

[16] M S Osman, A Korkmaz, H Rezazadeh, et al. *The unified method for conformable time fractional Schrödinger equation with perturbation terms*, Chin J Phys, 2018, 56(5): 2500-2506.

[17] M Rani, N Ahmed, S S Dragomir, et al. *Some newly explored exact solitary wave solutions to nonlinear inhomogeneous Murnaghan's rod equation of fractional order*, J Taibah Univ Sci, 2021, 15(1): 97-110.

[18] S Saha Ray, S Sahoo. *Comparison of two reliable analytical methods based on the solutions of fractional coupled Klein-Gordon-Zakharov equations in plasma physics*, Comput Math Math Phys, 2016, 56(7): 1319-1335.

[19] S Saha Ray, S Sahoo. *Traveling Wave Solutions to Riesz Time-Fractional Camassa-Holm Equation in Modeling for Shallow-Water Waves*, J Comput Nonlinear Dyn, 2015, 10(6): 061026.

[20] S Saha Ray, S Sahoo. *Two reliable efficient methods for solving time-fractional coupled Klein-Gordon-Schrödinger equations*, Appl Math Inf Sci, 2016, 10(5): 1799-1810.

[21] N Raza, M H Rafiq, M Kaplan, et al. *The unified method for abundant soliton solutions of local time fractional nonlinear evolution equations*, Results Phys, 2021, 22: 103979.

[22] S T R Rizvi, A R Seadawy, M Younis, et al. *Soliton solutions, Painleve analysis and conservation laws for a nonlinear evolution equation*, Results Phys, 2021, 23: 103999.

[23] S Sahoo, S Saha Ray. *A novel approach for stochastic solutions of wick-type stochastic time-fractional Benjamin–Bona–Mahony equation for modeling long surface gravity waves of small amplitude*, Stoch Anal Appl, 2019, 37(3): 377-387.

[24] S Sahoo, S Saha Ray, S Das. *An efficient and novel technique for solving continuously variable fractional order mass-spring-damping system*, Eng Comput, 2017, 34(8): 2815-2835.

[25] S Sahoo, S Saha Ray. *New travelling wave and anti-kink wave solutions of space-time fractional (3+1)-dimensional Jimbo-Miwa equation*, Chin J Phys, 2020, 67: 79-85.

[26] M Savescu, Q Zhou, L Moraru, et al. *Singular optical solitons in birefringent nano-fibers*, Optik, 2016, 127(20): 8995-9000.

[27] R Silambarasan, H M Baskonus, H Bulut. *Jacobi elliptic function solutions of the double dispersive equation in the Murnaghan's rod*, Eur Phys J Plus, 2019, 134: 125.

[28] A Tripathy, S Sahoo. *New Exact Solutions of (2+1)-Dimensional vDJKM and (3+1)-Dimensional BLMP Equations*, Int J Appl Comput Math, 2021, 7: 176.

[29] A Tripathy, S Sahoo. *Exact solutions for the ion sound Langmuir wave model by using two novel analytical methods*, Results Phys, 2020, 19: 103494.

[30] H Xin. *Optical envelope patterns in nonlinear media modeled by the Lakshmanan-Porsezian-Daniel equation*, Optik, 2021, 227: 165839.

[31] G Yel. *New wave patterns to the doubly dispersive equation in nonlinear dynamic elasticity*, Pramana - J Phys, 2020, 94: 79.

[32] C Yue, M Peng, M Higazy, et al. *Exploring the wave solutions of a nonlinear non-local fractional model for ocean waves*, AIP Adv, 2023, 13(5): 055121.

[33] C Yue, M Peng, M Higazy, et al. *Modeling of plasma wave propagation and crystal lattice theory based on computational simulations*, AIP Adv, 2023, 13(4): 045223.

[1]Department of Mathematics, School of Engineering, Presidency University, Bangalore, Karnataka-560064, India.

Email: tripathyananya3@gmail.com

[2]Kalinga Institute of Industrial Technology, Deemed to be University, Bhubaneswar, Odisha-751024, India.

Email: subha.bapi25@gmail.com